Journal of Applied Polymer Science

Investigations on the surface structure and properties of silica-polyamine composites on the nanoscales and microscales

Geoffrey Abbott, Robert Brooks, Edward Rosenberg
Department of Chemistry and Biochemistry, University of Montana, Missoula, MT 59812
Correspondence to: E. Rosenberg (E-mail: edward.rosenberg@mso.umt.edu)

ABSTRACT: The structure and properties of silica polyamine composites (SPC) made from microparticles of amorphous silica gel (300–600 microns) and silica nanoparticles (10–20 nm) modified with aminopropyltrimethoxysilane (APTMS), poly(allylamine) (PAA) or poly(ethyleneimine) (PEI) have been studied. The APTMS nano-hybrids showed batch capacities for copper equal to or better than the corresponding polymer-based micro-hybrids. Loading of the PEI on the nanoparticles was independent of molecular weight of the polymer. Dynamic light scattering measurements showed that the SiO_2 nanoparticles and the composites made from them aggregate in water and the degree of aggregation is dependent on the surface modification. All of the amine-modified materials were catalysts for the Knoevenagel reaction but interestingly, the microparticles modified with APTMS were better catalysts than the corresponding nanoparticles or the polyamine modified composites. Solid-state ^{19}Si NMR has been used to elucidate the surface structure of the various composites. © 2015 Wiley Periodicals, Inc. J. Appl. Polym. Sci. **2015**, *132*, 42271.

KEYWORDS: hydrophilic polymers; nanoparticles; nanowires and nanocrystals; supramolecular structures

Received 20 February 2015; accepted 26 March 2015
DOI: 10.1002/app.42271

INTRODUCTION

Solid phase hybrid materials are finding an increasingly wide range of applications in device design, environmental monitoring, separations science and catalysis.[1–11] Amorphous silica gels and sol-gels combined with polymers define a major portion of these hybrid materials for all these applications.[2–4,6–9] These silica based organic–inorganic materials offer a rigid matrix with high porosity and good thermal stability.[10,11] Most recently, there has been an enormous effort to bring these solid phase hybrid materials to the nanoscale. These efforts have met with considerable success in several different areas, namely nano-catalysis, sol-gel routes to hybrid materials, and optical devices.[12–16]

Our own interests in the area of organic–inorganic hybrid materials have centered on the subfield of silica–polyamine composites (SPC), an area that has also received much attention from other research groups.[17–21] Our initial investigations began in the early 1990's and focused on developing a metal remediation technology that was capable of being commercialized using the SPC platform. Eventually, this surface was expanded to a wider range of applications and synthetic approaches.[22–53] The early years focused on the synthesis and applications of the polyamine-amorphous silica gel composites to problems in heavy metal ion removal and recovery.[22–25,28–33] Later characterization of the polymer-surface interface and refining the use of polymer modifying ligands to improve metal selectivity was the focus of the research.[35–44] Most recently, the emphasis has been on the synthesis of these composites by more environmentally benign routes, the development of materials that can capture anions as well as cations and to their applications in catalysis.[45–53] Several of the SPC have been scaled-up and are being commercialized by Johnson–Matthey Ltd. for use in metal recovery and remediation in the mining industry.[31] SPC offer several advantages over conventional ion exchange and chelator polymer-based resins including, better capture kinetics and no shrink-swell while undergoing changes in pH and ionic strength.[38]

A logical extension of this work is to try to transfer the composite technology to silica nanoparticles from the porous, amorphous silica microparticles currently in use. The nanoparticles are essentially nonporous but have the same density of surface hydroxyl groups as amorphous silica gels (4.5–5.7 OH groups/nm^2).[54] The more porous amorphous silica microparticles may offer greater accessibility to active sites while the nanoparticles offer greater total surface area per unit volume or mass. Our initial studies in exploring these differences used the simpler

Additional Supporting Information may be found in the online version of this article.

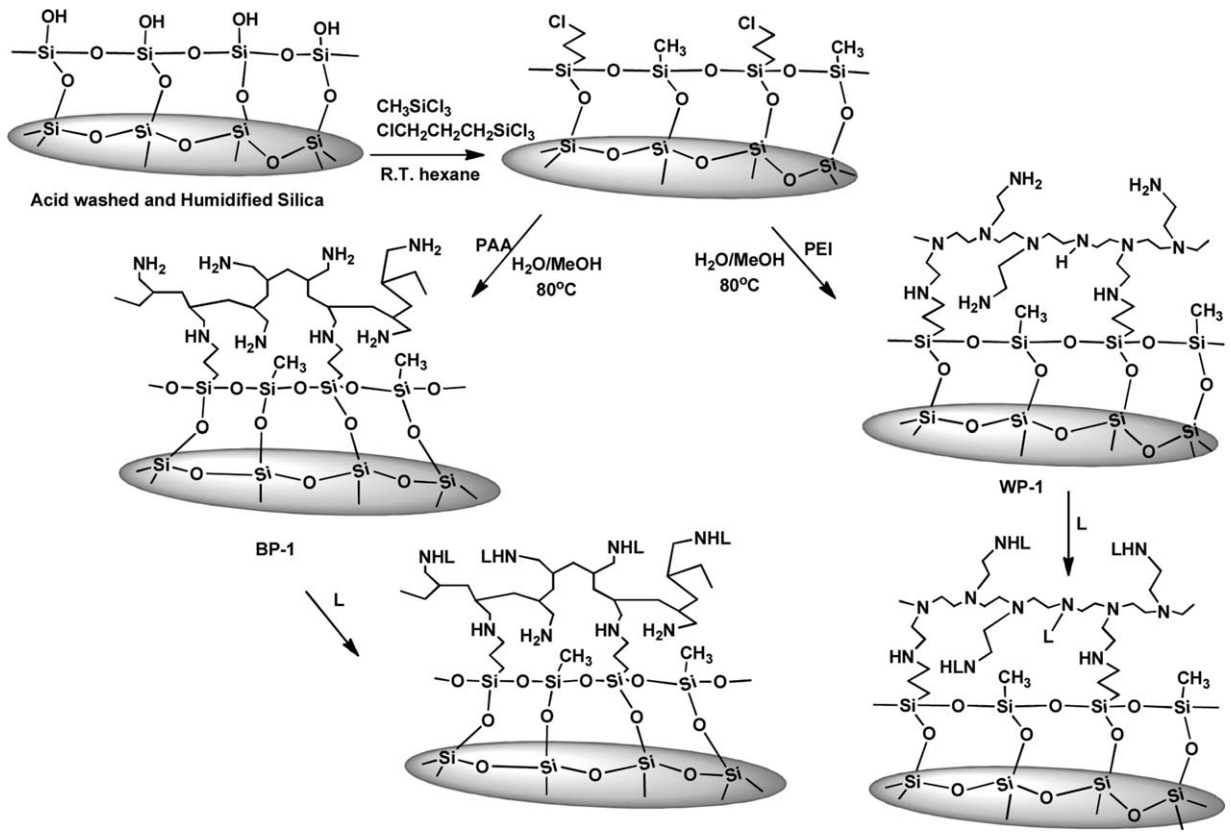

Figure 1. Scheme for synthesis of the silica polyamine composites.

aminopropyl functionality instead of the polyamine and this in turn offered the opportunity of exploring the actual role of the polymer, relative to the total number of amine sites with regard to capacity, durability and catalytic activity. The synthetic scheme for making the SPC is shown in Figure 1.

EXPERIMENTAL

Materials

The SPC, BP-1 and WP-1 microparticles were synthesized by previously reported procedures.[22–25] The SiO_2 nanoparticles (10–20 nm) (Aldrich) were dried at ~200° before use. Poly(allylamine) **(PAA)** (PolySciences) and poly(ethyleneimine) (Aldrich) and the monomers 3-aminopropyltrimethoxy- and methyltrimethoxysilane (Alfa Aesar) were used as received. Toluene (reagent grade, VWR) was dried over Type 4A molecular sieves (VWR) and methanol was used as received.

Stock solutions of Cu^{2+} were prepared using $Cu(SO_4)\cdot 10\ H_2O$. Solution pH was adjusted from the intrinsic pH, where necessary, using hydrochloric acid or sodium hydroxide. Stripping and recovery of copper was achieved with $2M\ H_2SO_4$. Metal standards for AA analyses were obtained from Fisher Scientific Co.

Methods

Solid State ^{13}C and ^{29}Si CPMAS NMR were performed on a 500 MHz Varian spectrometer operating at 125 and 99.4 MHz, respectively. A 4 mm rotor was used at spin speeds of 5–10 KHz with TANCP for cross polarization. IR spectra were taken on a Thermo-Nicolet 633 FT-IR spectrometer as KBr pellets.

Transmission Electron Microscopy (TEM) was performed on a Hitachi H-7100. Samples were prepared by incorporating the nanoparticles in an epoxy plug, after curing, thin slices were shaved off and the TEM taken on a selection of the slices.

Atomic Absorption (AA) analyses were done on an S series Thermo Electron corporation AA spectrometer. Metal ion solutions were run in a 2% nitric acid solution and were diluted to give approximately 0.1–0.2 absorbance units. AA analysis was used to determine the metal ion remaining bound on the surface of composites by measurement of the difference between the total metal ion in the initial solution and the total metal ion in the filtrate and rinses.

Synthesis

Synthesis of 3-Aminopropyl Trimethoxysilane (APTMS)-Coated Microparticles.[55] One gram of dried SiO_2 microparticles were top stirred in a solution of 10% (v/v) 3-aminopropyltrimethoxysilane in toluene for 30 min at room temperature. After stirring the particles were removed by filtration and washed by stirring with toluene for 1 h, which was repeated 3x, followed by drying under vacuum. $^{13}C\{^1H\}$ SS CPMAS NMR δ 11.3(C_1), 21.8(C_2), 44.3(C_3).

Synthesis of 3-Aminopropyl Trimethoxysilane (APTMS)-Coated Nanoparticles. One gram of dried SiO_2 nanoparticles were sonicated in a solution of 10% (v/v) 3-aminopropyltrimethoxysilane, in toluene, for 30 min at room temperature. After sonication the particles were removed by centrifugation and washed 3x by sonicating with toluene,

Table I. Comparison of the Properties of Micro- and Nano-SPC

SPC	Functional	Particle size	MW	%N	Cu Capacity Mmol g^{-1}	N:Cu ratio#
WP-1	PEI	150–300 μm	25k	3.10	1.1	1.8
BP-1	PAA	150–300 μm	15k	2.31	1.6	1.1
Nano-APTMS	APTMS	10–20 nm	-	3.21	1.4	1.6
Micro-APTMS	APTMS	10–20 nm	-	2.37	1.2	1.4
Nano-WP-1	PEI	10–20 nm	25k	3.82	0.6	4.5
Nano-BP-1	PAA	10–20 nm	15k	3.02	2.1	1.4

followed by drying under vacuum. $^{13}C\{^1H\}$ SS CPMAS NMR δ 11.5(C_1), 21.6(C_2), 44.3(C_3).

Synthesis of 7 : 1 Methyltrimethoxysilane (MTMS) : Chloropropyltrimethoxysilane (CPTMS)-Coated Nanoparticles. One gram of dried SiO_2 nanoparticles was suspended in 20 mL of 10%(v/v) 7 : 1 MTMS (1.75 mL):CPTMS (.25 mL) in toluene in a 50 mL Schlenk tube. The reaction mixture was then sonicated for 30 min at R.T. After completion, the nanoparticles were centrifuged out of the mixture at 16,000 rpm and washed. Washing was performed 3x by re-suspending the nanoparticles in ~20 mL of toluene and followed by centrifugation. After washing the nanoparticles were spun down and dried on a vacuum line. IR in KBr: 3399 (b), 2950 (w), 1625 (m), 1080 (s,b) $^{13}C\{^1H\}$ SSNMR δ 44.8 (C_3), 24.3 (C_2), 8.6 (C_1), −6.0 (Si-Me) cm^{-1}.

Synthesis of WP-1 [Poly(ethyleneimine)-(PEI)] Coated Nanoparticles. One gram of 7 : 1 MTMS:CPTMS coated nanoparticles were suspended in 1–2 mL of an 18% (w/w) aqueous 300 MW, 600 MW, 1200 MW, 1800 MW, 10,000 MW, and 25,000 MW PEI solution, with 1–2 mL of MeOH. The reaction mixture was then sonicated at R.T. for 24 h. The nanoparticles were then centrifuged at 16,000 rpm and the supernatant was poured off. The nanoparticles were washed 2x in ~20 mL of a 1 : 1 mixture of DI H_2O:MeOH, and 1x with DI H_2O only, by re-suspending the particles and spinning them back down. After washing, the particles were spun down and dried on a vacuum line. $^{13}C\{^1H\}$ SS CPMAS NMR δ 44.8 (C_3), 24.3 (C_2), 8.6 (C_1), 50–15 (Polymer), −6 (Si-Me).

Synthesis of BP-1 [Poly(allylamine)(PAA)]-Coated Nanoparticles. One gram of 7 : 1 MTMS : CPTMS coated nanoparticles were suspended in 1–2 mL of a 15% (w/w) aqueous 15,000 MW PAA solution, with 1–2 mL of MeOH. The reaction mixture was then sonicated at RT for 24 h. Upon completion the nanoparticles were centrifuged out of the solution at 16,000 rpm and the supernatant was poured off. The nanoparticles were washed 2x in ~20 mL of a 1 : 1 mixture of DI H_2O : MeOH, and 1x with DI H_2O only, by re-suspending the particles and spinning them back down. After washing, the particles were spun down and dried on a vacuum line. $^{13}C\{^1H\}$ SSNMR δ 44.8 (C_3), 24.3 (C_2), 8.6 (C_1), 50–15 (Polymer), −6 (Si-Me).

Equilibrium Batch Experiments for Determining Copper Capacities

Copper batch capacity tests were conducted by adding 100 mg of **SPC** to 10 mL of metal solution at intrinsic pH (3.0–3-5). All batch experiments were done in triplicate. To ensure equilibration, the metal ion and **SPC** mixtures were placed in a shaker bath. After 24 h the mixtures were allowed to settle (microparticles) or were centrifuged (nanoparticles). The supernatant (20 mL) was preserved with a few drops of 2% nitric acid solution for analysis using the AA method.

Dynamic Light Scattering Measurements

Nanoparticle (NP) samples were weighed out in 25 mg batches for the 5 different surfaces. Each NP sample was initially added to 1 mL of MilliQ water filtered through a .2 μm syringe filter. After addition of water, the mixture was sonicated in a 40 KHz VWR Sonication Bath for ~16 h. After the sonication had properly suspended the NP's, the solution appeared homogeneous and 10 μL of the suspension was added to 990 μL of filtered MilliQ water in a separate vial. This vial was then sonicated for an additional 16 h. A third dilution, 10 μL of suspension into 990 μL of filtered MilliQ, was made and sonicated for ~4 h prior to measurement. The dynamic light scattering measurements were made on a Malvern Zetasizer NS, and the samples were under sonication until ~30 s before measurements began. Each sample underwent three measurements, consisting of between 12–15, 10 second scans. The data for each measurement was then compiled using the Malver Zetasizer software and presented as graphs (Supporting Information Figures S1–S4).

RESULTS AND DISCUSSION

Comparison of Metal Ion Capacities and Surface Structure

Our initial comparisons between the micro- and nano-SPC focused on the functionalization of 10–20 nm silica nanoparticles and 300–600 μm amorphous silica gel with aminopropyltrimethoxysilane (APTMS). The reactions were performed in dry toluene at room temperature using 10–15% by weight solution and reaction times of 30 min.[55] It was found that the micro- and nano-APTMS composites had fairly similar copper capacities, 1.2 and 1.4 mmol Cu^{2+} g^{-1} respectively but had significantly different nitrogen loadings, 2.37 and 3.21% N, respectively (Table I). The APTMS micro- and nano-SPC copper capacities compare favorably with the commercialized SPC, WP-1 and BP-1 made from 25k MW poly(ethyleneimine) (PEI) and 15k poly(allylamine) PAA respectively.[35] The difference in copper loading is relatively small (16%) compared with the difference in nitrogen content (35%) for the micro and nanoparticles respectively. This suggests that not all the amine groups on the nano-APTMS are being utilized. The lower N/Cu ratio of 1.4 for micro-APTMS versus 1.6 for nano-APTMS also

supports the idea of many unused amine groups on the nano-APTMS and these values are intermediate between the N/Cu on the micro-SPC made with PEI (1.8) and PAA (1.0) (Table I).

Synthesis of the polymer-based nano-SPC was performed using procedures similar to those used of the micro-WP-1 and BP-1 except that the reaction mixtures were sonicated prior to and during reaction with the polymer in order to individualize the nanoparticles.[22–25] As for the micro-SPC, where a 7 : 1 mixture of methyltrichlorosilane (MTCS) and chloropropyltrichlorosilane (CPTCS) was used in the silanization step, the same ratio of methyltrimethoxysilane (MTMS) to chloropropyltrimethoxysilane (CPTMS) was used in the silanization step of the silica nanoparticles (Figure 1).[36] The nano-BP-1 and the nano-WP-1 both show a 0.7% increase in nitrogen content relative to their micro-analogues. (Table I). The total N content is higher for the WP-1 because of the higher N content of the monomer (33% in PEI versus 25% in PAA). The copper capacity of nano-BP-1 is higher than the micro-BP-1, being 2.1 and 1.6 mmol Cu^{2+} g^{-1} respectively, and the N/Cu for these two composites are closer at 1.4 and 1.1 respectively. Thus, the surface coordination sites for both composites are fairly similar. On the other hand, micro- WP-1 and nano-WP-1 have very different copper capacities of 1.1 and 0.6 mmol Cu $^{2+}$ g^{-1}. The higher N/Cu reported here is likely due to the fact that many of the amine groups of the surface-bound PEI are not used for metal binding as observed for nano-APTMS.

The high molecular weight PEI used in the nano-WP-1 reported in Table I is the same as that used for the commercially produced SPC. In the case of micro-WP-1, we previously found that the Cu^{2+} capacity and the nitrogen content were insensitive to the molecular weight of the PEI used to make the SPC.[35] We performed a similar study with the silica nanoparticles after silanization because we were concerned that the higher molecular weights might cause aggregation with nanoparticle SPC. This was not the case, however, as long, as the reactions were sonicated during reaction of the silanized silica nanoparticles with the polyamines. The results of this series of reactions between PEI of various molecular weights and silica nanoparticles that were silanized in the usual manner are summarized in Table II. The copper capacities vary only slightly (0.48–0.64 mmol Cu^{2+} g^{-1}) and all are well below the capacities observed for the same range of molecular weights for micro-SPC made with polyamines of different molecular weights.[32] Again, this is indicative of the fact that on the silanized silica nanoparticles a significant % of the amine groups are not involved in metal bonding and this contrasts sharply with micro-SPC made with PEI where the same insensitivity to MW was observed but where capacity increased significantly %N.[31,32] Thus surface loading of the PEI takes place in a similar way for both the micro- and nano-SPC but the availability of the amine groups differs markedly. PAA comes in only one molecular weight and we include two examples of the nano-SPC, BP-1 in Table II, to illustrate the variation in Cu^{2+} capacity from two different runs and this gives evidence that the variation in the Cu^{2+} capacities for the PEI-SPC in Table II are probably within experimental error and/or are due to slight differences in experimental conditions. A transmission electron micrograph of PAA on silanized

Table II. Variation in Copper Capacities for Nano-SPC Made with PEI (MW=300-25k)

Polymer	mmol Cu/gram composite
PEI 300 MW	0.64
PEI 600 MW	0.55
PEI 1200 MW	0.54
PEI 1800 MW	0.48
PEI 10,000 MW	0.62
PEI 25,000 MW	0.61
PAA 15,000 MW	2.14
PAA 15,000 MW	2.04

silica nanoparticles (nano-BP-1) is shown in Figure 2. The particles do aggregate and it was decided to undertake the extent of aggregation using dynamic light scattering (DLS) on a selection of the composites to understand the relationship between the degree of aggregation and the surface of the composite. The results are summarized in Table III and the DLS graphs are given in the Supporting Information (Figures S1–S4).

Three measurements were made on each of four nano-SPC particles. The first was made within 30 s of stopping sonication and introduction into the DLS apparatus and at 2 min intervals after the initial scans. All the samples including the unmodified silica particles aggregate rapidly and aggregation increases with time, except for the case of WP-1(300 MW).

In all cases the distribution of particles becomes broader with time suggesting a re-equilibration of the aggregation process where some of the larger particles break up. The rate of this process is apparently faster for the lowest molecular weight SPC examined. Interestingly, the composite with the highest molecular weight polymer, PAA, showed the smallest aggregates. This suggests that achieving a free energy minimum with regard to hydrogen bonding controls aggregate size. The linear, higher molecular weight PAA has the primary amine groups extended

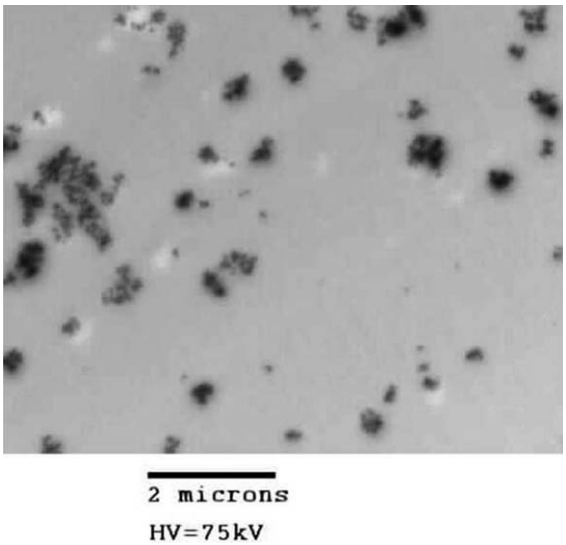

Figure 2. TEM of PAA on silanized silica nanoparticles (nano BP-1).

Table III. Dynamic Light Scattering for Nano-SPC Particles[a]

Substance	Measurement 1	Measurement 2	Measurement 3
SiO_2 (20 nm)	21.7	57.5	78.5
WP-1 (300 MW)	113	147	111
WP-1 (600 MW)	91.3	148	181
BP-1(11000 MW)	51.8	75.9	93.4

[a] ± 10%.

away from the polymer backbone and could provide more hydrogen bonds per unit area of surface. Assuming a monolayer of polymer-silane coating on the surface of the nanoparticle, we estimate a diameter of 25–30 nm for a single SPC nanoparticle, based on molecular modeling studies.[35] This means that BP-1 exists initially as a dimer while the WP-1 SPC particles exist mainly as tetramers to hexamers. Under sonication, we can only speculate that the particles are monomeric because it was not possible to measure DLS during sonication. That the WP-1 (300 MW) does not increase in aggregation on going from the second to the third DLS measurement is more difficult to rationalize. A possible explanation is that there is competition between hydrogen bonding with water and hydrogen bonding with the polymer amines for this lower molecular weight polymer and that equilibration is slow while hydrogen bonding with the amines is kinetically favored.

The robustness of the SPC is due at least, in part, to the multipoint anchoring of the polyamine to the silanized silica surface. In our prior work, we demonstrated that the use of a mixture of methyl- and chloropropylsilanes reduces the number of anchor points, without compromising long-term stability, while having the beneficial effect of increasing capacity and capture kinetics.[36,38] Here, we compare the number of anchor points for related micro- and nano-SPC and the impact of this feature on copper capacity (Table IV). Using the % N, corrected for mass gain, the molecular weight of the polymer and the chloride content before and after reaction with the polyamine we can calculate the number of anchor points, on average, per polymer molecule.[48,51] The PEI micro-SPC made with only chloropropylsilane has more anchor points than the related nano-SPC, with more utilization of chloride and a higher Cu^{2+} capacity. Taken together these differences define a more kinetically restricted surface environment for the nano-SPC made with PEI. The composites made with the linear polymer PAA have fewer anchor points than the SPC made with the branched polymer, PEI (Table IV). However, the nano-SPC made with only CPTMS and PEI has fewer anchor points than its micro analog while the related composite made with PAA has more anchor points than its micro analog. The nano-PEI has much lower chloride utilization as a result of the much larger loading of chloropropyl groups. Dilution of the chloropropyl groups with MTMS results in fewer anchor points, as expected, but here again the utilization of chloride groups is much lower for the nano-PEI than for the micro-PEI (Table IV). The last two entries in Table IV are the anchor point data for micro-SPC made by the sol-gel route using tetramethoxysilane (TMOS), MTMS and CPTMS in different ratios.[51] It can be seen that using higher ratios of TMOS leads to higher copper capacities and better chloride utilization. This is the result of making more bulk silica which has the effect of making more chloropropyl groups surface available.[30] In the case of the nano-SPC, it may be that the chloropropyl groups are adsorbed onto the surface of the particle making them less available for reacting with the polyamine.[48,51]

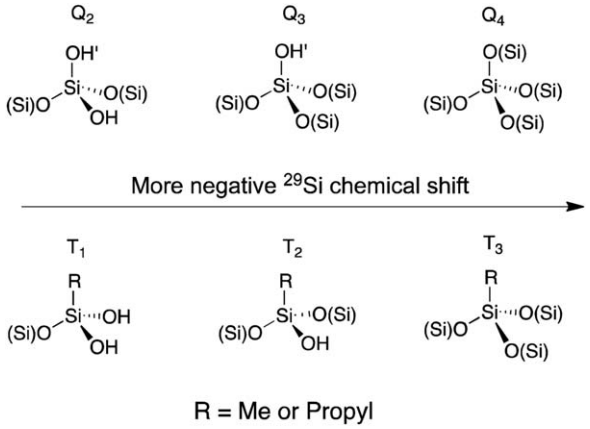

Chart 1. Surface silicon species on modified silicas.

Table IV. Anchor Points and Copper Capacities for Micro and Nano-SP

Material	Particle Size	Run No.	Reactant Conc.	%Conversion[a]	Rate Constant (M^{-1} s^{-1})	R^2
BP-1	Micro	1	0.1M	79	0.25	0.99
WP-1	Micro	1	0.1M	45	0.11	0.94
Aminopropyl	Micro	1	0.1M	95	0.5	0.97
Silica	Micro	1	0.1M	0	N/A	N/A
Aminopropyl	Nano[b]	1	0.1M	85	0.33	0.95
Silica	Nano	1	0.1M	0	N/A	N/A
BP-1	Micro	2	0.1M	24	0.056	0.81
Aminopropyl	Micro	2	0.1M	90	0.33	0.98

[a] Reactions were monitored for 1 h in toluene at room temperature using 0.1 g of catalyst.
[b] Nano-reaction was sonicated for 30 min before starting the reaction.

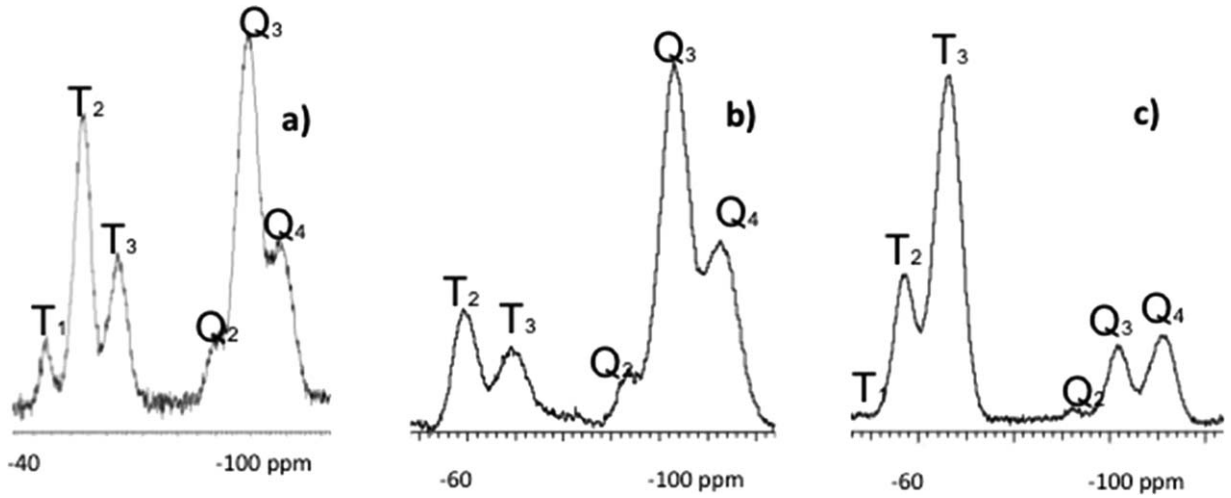

Figure 3. Solid-state CPMAS ^{29}Si NMR at 99.4 MHz of: (a) 20 nm silica nanoparticles reacted with 7 : 1 MTMS:CPTMS; (b) 300–600 μm amorphous silica silanized with 7 : 1 MTCS:CPTCS; (c) 300–600 μm silanized silica particles made by the sol-gel route using 62 : 30 : 1 TMOS: MTMS: CPTMS (Note: scales are slightly different).

Solid-state cross-polarization magic angle spinning (CPMAS) ^{29}Si NMR has proven to be an invaluable tool for analyzing the nature of the species on a surface-modified silica.[26] Specifically, the chemical shift is very sensitive to the number of OH groups on the silicon and to whether or not it has an attached alkyl group. Silicon atoms with an alkyl group have less negative chemical shifts and are designated as T_3, T_2, or T_1 sites depending on whether they have 0, 1, or 2 OH groups respectively (Chart 1). Similarly, silicon atoms with no alkyl groups come at more negative chemical shifts than the T sites and are designated as Q_4, Q_3, or Q_2 depending on whether they have 0, 1, or 2 OH groups (Chart 1).

C1

An examination of the solid-state NMR of the silica composites made from 10 to 20 nm silica, 300–600 μm silica and a silica composite made via the sol gel route, also 300–600 μm, reveals some interesting differences (Figure 3).

The most interesting difference is that only the nanoparticles show significant T_1 sites for the surface modified with a 7 : 1 ratio MTMS: CPTMS [Figure 3(a)]. This is consistent with the smaller radius of curvature of the nanoparticles that would tend to make reaction with more than one OH somewhat less likely. The ratio of T : Q is about 1 : 1 for the nanoparticles, as expected for this morphology, where the surface area and particle volume are usually the same. The spectrum for the 300–600 μm silanized amorphous silica gel (this is the precursor to commercialized SPC) shows the lowest ratio of T : Q sites, as expected for a material with more bulk silica, and more importantly, more T_2 than T_3 sites [Figure 2(b)]. The sol-gel sample, made with 62 : 30 : 1 TMOS, MTMS and CPTMS, shows the largest ratio of T : Q sites and the highest ratio of T_3 : T_2 sites suggesting that this synthetic option offers a more stable silanized surface relative to the nanoparticles [Figure 2(c)].[51] These

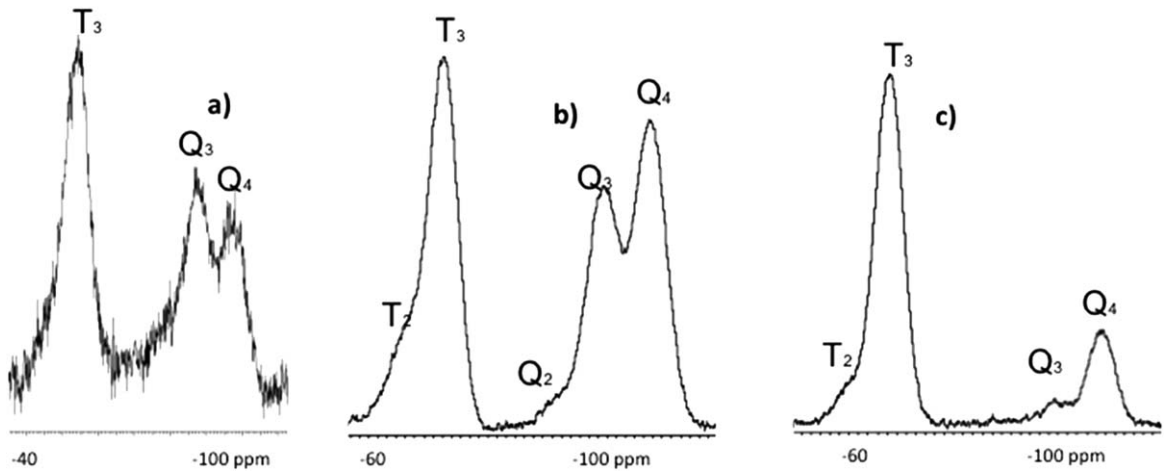

Figure 4. Solid-state CPMAS ^{29}Si NMR at 99.4 MHz of: (a) 20 nm silica nanoparticles reacted with 7 : 1 MTMS:CPTMS and then PAA at 80 C; (b) 300–600 μm amorphous silica silanized with 7 : 1 MTCS:CPTCS and then PAA at 80 C; (c) 300–600 silanized using silica particles made by the sol-gel route 62 : 30 : 1 TMOS : MTMS : CPTMS and then PAA at 80 C (Note: scales are slightly different).

Table V. Second-Order Rate Constants for the SPC-Catalyzed Knoevenagel Reaction

Composite	# Anchor points	% Cl utilized	Cu capacity (mg/g)
PEI CPTMS only nano	178	64	39
PEI CPTCS only micro	230	80	65
PAA CPTMS only nano	154	45	136
PAA CPTCS only micro	105	80	90
PAA 7 : 1 mix of CPTMS and MTMS nano	41	27	130
PAA 7 : 1 mix of CPTCS and MTCS only	24	81	100
PAA Sol-gel micro 4.5 : 1 : 1	38	38	100
PAA sol-gel micro 62 : 30 : 1	13	51	118

data point to the sol-gel material as the being the most stable material in the post silanization phase, but the economics of commercially producing the SPC materials via sol-gel chemistry may not be viable.

On reaction with PAA the surface features of the three silanized SPC change significantly (Figure 4). In all three cases the ratio of T_3 : T_2 has increased and in the case of the nanoparticles the T_1 sites have disappeared. We interpret this in terms of the polyamine-catalyzed reaction of surface hydroxyl groups with the alkyl-silanes.[51] Thus after reaction with the polyamine, surface reaction chemistry is driven towards completion and the ^{29}Si NMR suggests that all three routes eventually lead to SPC that should exhibit similar stability towards hydrolytic deterioration.[48–51]

Catalysis of the Knoevenagel Reaction by Micro- and Nano-SPC

It has long been known that amines catalyze the Knoevenagel reaction, which condenses an aldehyde or ketone with an activated methylene group to obtain highly substituted alkenes.[56]

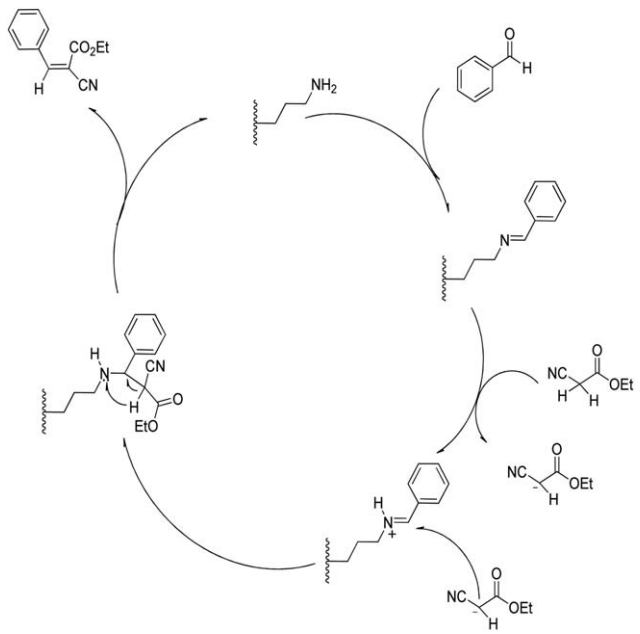

Figure 5. Mechanism of the Knoevenagel reaction as it occurs on SPC.

More recently, it was reported that the condensation of benzaldehyde with 2-cyano-ethylacetate could be catalyzed by amino propyl groups bound to the surface of mesoporous silica (Equation 1).[57]

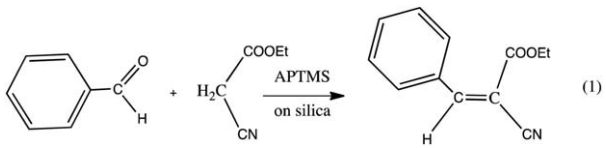

Based on these results we undertook a study of the heterogeneous amine catalysis of the reaction in Equation 1 using the nano- and micro-SPC discussed here for comparison with the prior work. The previous study reported only overall conversion to product but we thought it be interesting to compare the rate of catalysis for the APTMS-, PAA-(BP-1) and PEI-(WP-1) SPC for both the nano and microparticles. The results of this study are given in Table V. Second order behavior was assumed and reasonably good correlation coefficients were obtained from the least squares fit to the second order rate equation ($t_{(1/2)} = 1/k[B_0]$ out to 4 half lives. Several of the values were checked using the equation $[B] = 1/(1/[B_0] + kt)$), where B_0 is the initial concentration of aldehyde and B is the concentration of aldehyde at time t. All the reactions were run at room temperature using 0.1M solutions of the reactants in toluene and 0.1 g of the SPC. It can be seen that the best catalyst was the APTMS-micro, followed closely by APTMS-nano, BP-1-micro and then WP-1-micro. This order of activity can be understood in terms the formation of an intermediate imine of the aldehyde followed by reaction with the activated methylene (Figure 5).[55] The formation of the imine intermediate would be most favorable with the least encumbered amine and for the catalysts employed here the amino propyl group is the best choice. BP-1 with the primary amine extended off the backbone would be expected to be better than WP-1 where the amine is in the polymer backbone. That the APTMS-micro was significantly faster than the APTMS-nano can be attributed to the higher porosity of the micro-SPC and the apparently crowded environment of the nano-APTMS (*vide supra*). Second runs were done with the micro-APTMS and the micro-BP-1 and it can be seen that the APTMS held its reactivity and conversion efficiency much better than BP-1. This can be attributed to the formation of imine intermediates that are too sterically encumbered to

react with the activated methylene in the nucleophile. This interpretation is consistent with the very low rate constant for the second micro-BP-1 run. In our prior work, a particular stability of the imine intermediates of the PAA bound imine has been noted.[27,45]

CONCLUSIONS

There are both similarities and differences when considering the properties of the micro- and nano-SPC. Copper capacities are quite comparable for the APTMS and PAA modified micro and nanoparticles. The loading of PEI on both types of particles is relatively insensitive to the molecular weight of the polymer. On the other hand, the copper capacity for the nano-PEI-SPC is much lower than the micro-analog as is the utilization of the chloropropyl groups. This has been interpreted here as a consequence of a more crowded surface that results in fewer kinetically accessible amine sites for this branched polymer. This kind of steric effect is also seen in the relative rates of catalysis of the Knoevenagel reaction where the micro-APTMS gives faster rates than its nano-analog. We attribute this to the smaller radius of curvature expected for the nano-APTMS which causes unwanted contact with the surface that results in hydrolysis.[57]

Taken together the main conclusion from this work is that in many instances including catalysis the overall larger surface area available with nanoparticles does not always give the best result. In the case of surface-modified nanoparticles local environments appear to be a deciding factor in determining the physical and chemical properties of the SPC surface.

ACKNOWLEDGMENTS

The authors wish to thank the National Science Foundation (CHE – 1049569) for generous support of this research.

REFERENCES

1. Huang, Y. G.; Jiang, F.-L.; Hong, M. C. *Coord. Chem. Rev.* **2009**, *253*, 2814.
2. Yuan, L.; Zhao, L.; Liu, N.; Wei, G.; Zhang, Y.; Wang, Y.; Yu, C. *Chem. Eur. J.* **2009**, *15*, 11319.
3. Carniato, F.; Secco, A.; Gatti, G.; Marchese, L.; Sappa, E. *Sol-Gel Sci. Technol.* **2009**, *52*, 235.
4. Banet, P.; Griesmar, P.; Serfaty, S.; Vidal, F.; Jaouen, V.; Le Huerou, J. Y. *J. Phys. Chem. B* **2009**, *113*, 14914.
5. Srivastava, S.; Gaubert, G.; Pucheault, M.; Vaultier, M. *Chem. Cat. Chem.* **2009**, *1*, 94.
6. Kang, D. J.; Bae, B. S. *Acc. Chem. Res.* **2007**, *40*, 903.
7. Dunn, B.; Zink, J. *Acc. Chem. Res.* **2007**, *40*, 729.
8. Ashkenasy, D.; Cahen, R.; Cohen, A.; Shanzer, A.; Vilan, A. *Acc. Chem. Res.* **2002**, *35*, 121.
9. Tezuka, T.; Tadanaga, K.; Hayashi, A.; Tatsumisago, M. *J. Am. Chem. Soc.* **2006**, *128*, 16470.
10. Mark, J. E.; Lee, C.; Bianconi, P. A. Hybrid Inorganic-Organic Composites, ACS Symposium Series 585, Washington, DC, **1995**.
11. Nalwa, H. S. Handbook of Organic-Inorganic Hybrid Materials and Nanocomposites. 2-Volume Set; American Science Publishers: Stevenson Ranch, CA, **2003**.
12. Wang, Y. B.; Li, L.; Zhang, H.; Song, H. *Langmuir* **2009**, *29*, 1273.
13. Kasinathan, P.; Yoon, J. W.; Hwang Dong, W.; Lee, U. H.; Hwang, J. S.; Hwang, Y. K.; Chang, J. S. *Appl. Catal. A: Gen.* **2013**, *451*, 236.
14. Adam, F.; Appaturi, J. N.; Khanam, Z.; Thankappan, Z.; Nawi, R.; Asri, M. *Appl. Surf. Sci.* **2013**, *264*, 718.
15. Khdary, N. H.; Ghanem, M. A. *J. Mater. Chem.* **2012**, *22*, 12032.
16. Tu, H. L.; Tsai, F. Y.; Mou, C. Y. *J. Mater. Chem.* **2008**, *18*, 1771.
17. Crane, L. J.; Kakodkar, V. U.S. Pat. 5,092,992 (**1992**).
18. Plueddemann, E. P. U.S. Pat. 4,379,931 (**1983**).
19. Dias, N. L.; Filho, Y. G. *Sep. Sci. Technol.* **1997**, *32*, 2335.
20. Mahmoud, M. E.; Soliman, E. M. *J. Liquid Chromatogr. Relat. Technol.* **2003**, *26*, 3045.
21. Soliman, E. M. *Anal. Lett.* **1996**, *30*, 1739.
22. Pang, D.; Rosenberg, E. U.S. Pat. 5,695,882 (**1997**).
23. Pang, D.; Rosenberg, E. U.S. Pat. 5,997,748 (**1999**).
24. Fischer, R. J.; Rosenberg, E. U.S. Pat. 6,576,590 (**2003**).
25. Fischer, R. J.; Rosenberg, E. U.S. Pat. 7,008,601 (**2006**).
26. Wong, Y. O.; Maranda, P.; Rosenberg, E. U.S. Pat. 8,343,446 (**2012**).
27. Beatty, S. T.; Fischer, R. J.; Rosenberg, E.; Pang, D. *Sep. Sci. Technol.* **1999**, *34*, 2723.
28. Beatty, S. T.; Fischer, R. J.; Rosenberg, E.; Pang, D. *Sep. Sci. Technol.* **1999**, *34*, 3125.
29. Beatty, S. T.; Fischer, R. J.; Rosenberg, E.; Hagars, D. L. *Ind. Eng. Chem. Res.* **1999**, *38*, 4402.
30. Rosenberg, E.; Fischer, R. J.; Deming, J.; Anderson, C. Silica Polyamine Composites as Platforms for Green Ore Processing. In ALTA 2000 Technical Proceedings, Perth, Australia, SX/IX-1, ALTA Metallurgical Services.
31. Rosenberg, E.; Fischer, R. J.; Deming, J.; Hart, C. K.; Miranda, P.; Allen, B. Silica Polyamine Composites: Advanced Materials for Heavy Metal Recovery, Recycling and Removal. In Symposium Proceedings of the International Conference on Materials and Advanced Technologies; White, T., Sun, D., Eds.; Materials Research Society: Singapore, **2001**; Vol. I, p 173.
32. Anderson, C.; Rosenberg, E.; Hart, C. K.; Ratz, L.; Cao, Y. Single Step Separation and Recovery of Palladium Using Nitrogen Species Catalyzed Pressure Leaching and Silica Polyamine Composites. In Proceedings of the 5th International Symposium on Hydrometallurgy. Volume 1: Leaching and Purification;Young, C., Ed. TMS: Warendale, PA, 2003; p 393.
33. Rosenberg, E.; Nielsen, D.; Miranda, P.; Hart, C. K.; Cao, Y. Silica Polyamine Composites: Advanced Materials for Ion Recovery and Remediation. In Proceedings of the 66th Annual International Water Conference, Orlando, FL, IWC-05–40, **2005**.

34. Hughes, M.; Miranda, P.; Nielsen, D.; Rosenberg, E.; Gobetto, R.; Viale, A.; Burton, S. In Recent Advances and Novel Approaches in Macromolecule-Metal Complexes; Barbucci, R., Ciardelli, F., Ruggeri, G., Eds.; Wiley-VCH (Macromolecular Symposia 235): Weinheim, **2006**; p 161.
35. Rosenberg, E. In Macromolecules Containing Metal and Metal-like Elements; Abd-El-Aziz, A., Carraher, C. C., Pittman, C. U., Zeldin, M., Eds.; Wiley-Interscience: Hoboken, NJ, **2005**; Vol. 4, p 51.
36. Hughes, M.; Nielsen, D.; Rosenberg, E.; Gobetto, R.; Viale, A.; Burton, S. *Ind. Eng. Chem. Res.* **2006**, *45*, 6538.
37. Hughes, M.; Rosenberg, E. *Sep. Sci. Technol.* **2006**, *42*, 261.
38. Rosenberg, E.; Hart, C. K.; Hughes, M.; Kailasam, V.; Allen, J.; Wood, J.; Cross, B. Performance Improvement Through Structural Design and Comparison with Polystyrene Resins of Silica Polyamine Composites. In Proceedings of the 67th International Water Conference, Pittsburgh, PA, IWC-06–34, **2006**.
39. Bandosz, T. J.; Seredych, M.; Allen, J.; Wood, J.; Rosenberg, E. *Chem. Mater.* **2007**, *19*, 2500.
40. Gleason, W.; Rosenberg, E.; Sharmin, A.; Hughes, M. Coordination analysis of Silica Polyamines by FT-IR. In Proceedings of SME (Society for Mining, Metallurgy and Exploration) Hydrometallurgy Conference, Phoenix, Arizona, **2008**.
41. Hughes, M.; Wood, J.; Rosenberg, E. *Ind. Eng. Chem. Res.* **2008**, *47*, 6765.
42. Rosenberg, E.; Hughes, M.; Wood, J. Structural Design of Nanoporous Silica Polyamine Composites for Metal Separations in Water. In Proceedings of the 68th International Water Conference, Orlando, Florida, October 21–25, **2007**. IWC-07–16.
43. Nielsen, D.; McKenzie, J.; Clancy, J.; Rosenberg, E. *Chim. Oggi* **2009**, *26*, 42.
44. Allen, J.; Rosenberg, E.; Chierotti, M. R.; Gobetto, R. *Inorg. Chim. Acta* **2010**, *363*, 617.
45. Wong, Y. O.; Miranda, P.; Rosenberg, E. *J. Appl. Polym. Sci.* **2010**, *115*, 2855.
46. Karakhanov, E. A.; Maximov, A. L.; Zatolochnaya, O. V.; Rosenberg, E.; Hughes, M.; Kailasam, V. *Petrol. Chem.* **2009**, *49*, 107.
47. Allen, J.; Rosenberg, E.; Karakhanov, E. A.; Kardashev, S. V.; Maximov, A.; Zolotukhina, A. *Appl. Organomet. Chem.* **2011**, *25*, 245.
48. Allen, J.; Berlin, M.; Hughes, M.; Johnston, E.; Kailasam, V.; Rosenberg, E.; Sardot, T.; Wood, J. *Mat. Chem. Phys.* **2011**, *126*, 973.
49. Berlin, M.; Allen, J.; Kailasam, V.; Rosenberg, E. *Appl. Organomet. Chem.* **2011**, *25*, 530.
50. Karakhanov, E. A.; Maximov, A. L.; Kardasheva, A.; Zolotukhina, A.; Rosenberg, E.; Allen, J. *Macromol. Symp. (Macromolecular Complexes)* **2011**, *304*, 55.
51. Allen, J.; Johnston, E.; Rosenberg, E. *ACS Appl. Mater. Interf.* **2012**, *4*, 1573.
52. Rosenberg, E.; Hart, C. K. Mine Waste Clean up with Novel Organic-Inorganic Hybrid Materials. In Proceedings of 72nd International Water Conference, Orlando, FL, **2011**; p 153.
53. Kailasam, V.; Rosenberg, E. *Hydrometallurgy* **2012**, *129-130*, 97.
54. Fletcher, P. D. I.; Holt, B. K. *Langmuir* **2011**, *27*, 12869.
55. Kim, T. W.; Chung, P.-W.; Victor, S.-Y.; Lin, V. S.-Y. *Chem. Mater.* **2010**, *22*, 5093.
56. House, H. O. Modern Synthetic Reactions, 2nd Ed.; W. A. Benjamin: Menlo Park, CA, **1972**; p 646.
57. Wang, S. G. *Catal. Commun.* **2003**, *4*, 469.